Published in final edited form as:
Pain. 2014 June ; 155(6): 1150–1160. doi:10.1016/j.pain.2014.03.003.

Differential Distribution of PI3K Isoforms in Spinal Cord and Dorsal Root Ganglia: Potential Roles in Acute Inflammatory Pain

Mathias Leinders[1,*], **Fred J. Koehrn**[1], **Beatrix Bartok**[2], **David L. Boyle**[2], **Veronica Shubayev**[1,3], **Iveta Kalcheva**[2], **Nam-Kyung Yu**[4], **Jihye Park**[4], **Bong-Kiun Kaang**[4], **Michael P. Hefferan**[5], **Gary S. Firestein**[2], and **Linda S. Sorkin**[1]

[1]Department of Anesthesiology, University of California, San Diego, La Jolla, CA 92093, USA

[2]Deprtment of Medicine, Division of Rheumatology, University of California, San Diego, La Jolla, CA

[3]San Diego VA Healthcare System, La Jolla, CA

[4]Department of Biological Sciences and Brain and Cognitive Sciences, Seoul National University, Seoul 151-747, Korea

[5]Neuralstem Inc., Rockville, MD 20850, USA

Abstract

PI3-kinases (PI3Ks) participate in nociception within spinal cord, dorsal root ganglion (DRG) and peripheral nerves. To extend our knowledge, we immunohistochemically stained for each of the four Class I PI3K isoforms along with several cell specific markers within lumbar spinal cord, DRG and sciatic nerve of naïve rats. Intrathecal and intraplantar isoform specific antagonists were given as pre-treatments before intraplantar carrageenan; pain behavior was then assessed over time. The α-isoform was localized to central terminals of primary afferent fibers in spinal cord laminae IIi-IV as well as to neurons in ventral horn and DRG. The PI3Kβ isoform was the only Class I isoform seen in dorsal horn neurons, it was also observed in DRG, Schwann cells and axonal paranodes. The δ-isoform was found in spinal cord white matter oligodendrocytes and radial astrocytes, while the γ-isoform was seen in a subpopulation of IB4-positive DRG neurons. No isoform co-localized with microglial markers or satellite cells in naïve tissue. Only the PI3Kβ antagonist, but none of the other antagonists, had anti-allodynic effects when administered intrathecally; coincident with reduced pain behavior, this agent completely blocked paw carrageenan-induced dorsal horn 2-amino-3-(3-hydroxy-5-methylisoxazol- 4-yl) propanoic acid (AMPA) receptor trafficking to plasma membranes. Intraplantar administration of the γ-antagonist

Corresponding author: Linda S. Sorkin, PhD, 9500 Gilman Drive, La Jolla, CA 92093-0818; Tel: 619-543-3498, Fax: 619-543-6070, lsorkin@ucsd.edu.
*present address:
Department of Neurology, University of Wurzburg, Josef-Schneider-Str. 11, 97080 Wurzburg, Germany

Conflict of interest statement
The authors have no conflicts of interest to report.

prominently reduced pain behavior. These data suggest that each isoform displays specificity with regard to neuronal type as well as to specific tissues. Furthermore, each PI3K isoform has a unique role in development of nociception and tissue inflammation.

Keywords

inflammation; allodynia; carrageenan; GluA1 trafficking; Schwann cell; PI3Kinase

Introduction

Phosphoinositide 3-kinases (PI3Ks) are dual lipid- and protein-signaling kinases involved in numerous cellular functions [1; 29; 40]. At the plasma membrane, they convert PIP2 to phosphatidylinositol-3,4,5-trisphosphate [PI(3,4,5)P3], which then induces downstream signaling events via various mediators and adaptor proteins, including AKT/PKB and mTOR [22]. Members of the PI3K signaling family differ in expression and substrate specificity and are separated into three classes. Class I isoforms have been studied most extensively: PI3Kα, PI3Kβ and PI3Kδ are activated by receptor tyrosine-kinases [23], while PI3Kγ is activated by G-protein-coupled receptors (GPCRs), including chemokine receptors, to regulate cellular functions such as cell survival, proliferation, migration and adhesion [39]. Class II and III PI3K differ from class I in structure and regulation and will not be discussed here, although one class II isoform has been implicated in spinal pain processing [2]. PI3Kα and PI3Kβ are ubiquitously expressed by most or all cell types [50], while PI3Kδ and PI3Kγ are predominantly found in cells with hematopoietic [39] and endothelial [38] lineage. More recently, the PI3Kδ isoform was identified as a critical isoform in mesenchymal cells, such as fibroblast-like synoviocytes [4]. Significantly, PI3Kδ is also expressed in brain and neuroblastoma cell lines and may participate in peripheral nerve regeneration following axotomy [18]. Localization of specific PI3K isoforms in spinal cord and dorsal root ganglia (DRG) is still largely unexplored and their roles are unknown; our data suggest that the aforementioned generalizations regarding widespread expression do not hold for these tissues, at least under naïve conditions.

A growing body of evidence indicates that pharmacological blockade of spinal PI3K attenuates inflammation/injury-induced hypersensitivity to cutaneous inflammation [11; 34; 47; 52]. Activity-induced trafficking of nociceptive receptors and channels, notably membrane insertion of TRPV1, ASIC1 and voltage gated calcium channels can be PI3K dependent [17; 44; 49; 54] and thus, may contribute to sensitization. In hippocampus, events downstream of PI3K activation can result in fast insertion of the 2-amino-3-(3-hydroxy-5-methylisoxazol- 4-yl) propanoic acid receptor (AMPAr) subunit, GluA1, into neuronal plasma membranes [26]. This process is essential to long-term potentiation [45].

PI3K signaling also has major importance in immunity, in part, through induction of inflammatory mediators. Indeed, dual PI3Kα/γ-inhibition decreases proinflammatory cytokine production elicited by tumor necrosis factor (TNF) or LPS in vitro [16], although in general, PI3Kδ and γ isoforms have predominant roles in inflammation. These isoforms can

have synergistic effects on cytokinemediated neutrophil-endothelium interactions [37], or can individually affect leucocyte chemotaxis [42] or endothelial leakage [31].

The role of PI3K signaling in nociceptive processing and in inflammatory processes is increasingly appreciated. However, little is known about individual isoform distribution in the nervous system or the relative contribution of each to nociceptive transmission during peripheral inflammation. In this study, we investigated cellular distribution of Class I PI3K isoforms in spinal cord and DRG in naive rats. Furthermore, we examined the effects of blocking individual isoforms via intrathecal and intraplantar administration of antagonists on pain behavior in a rat model of acute peripheral inflammation. In addition, we examined the ability of intrathecal isoform specific antagonists, which were antiallodynic, to block spinal GluA1 trafficking in the same inflammation model.

Methods

Adult male Holtzman rats (250-300g; Harlan Industries, Indianapolis, IN) were fed ad libitum and maintained under a 12h light/dark cycle; light on at 07:00h. Animals recovered from shipping for 2 days before use; on the day of the experiment, animals acclimated to the testing room for at least 1h prior to experimentation. All procedures were performed during the light cycle. Experiments were in compliance with the National Institutes of Health Guide for the Care and Use of Laboratory Animals, and the Institutional Animal Care and Use Committee of the University of California, San Diego, approved all animal protocols.

Quantitative real-time PCR (qPCR)

Rats were anesthetized with isoflurane and either allowed to wake up with no manipulation (N=3) or injected bilaterally in the plantar surface of both hindpaws with 150μl of 2% carrageenan prior to being placed in their home cages (N=4). After 4 h, rats were deeply re-anesthetized with isoflurane (5%) and transcardially perfused with room temperature (RT) sterile saline to minimize blood contamination of collected tissue. Spinal cords (L4-L6) were dissected and the dorsal half of the cords and the DRGs (L4 + L5) were separately snap frozen on dry ice. Messenger RNA for p110α, p110β, p110γ and p110δ subunits was quantified as previously described using Taqman PCR analysis and the GeneAmp 7300 Sequence Detection System [5]. Forward and reverse primers as well as fluorogenic TaqMan FAM/TAMRA-labeled hybridization probes were used (Assays on Demand; Applied Biosystems, Foster City, CA). To control for sample cellularity, HPRT forward and reverse primers and labeled probes were included in separate PCRs. Threshold C(t) values were normalized to a standard curve generated from serial dilutions of complementary DNA derived from rat Concovalin A stimulated peripheral blood mononuclear cells (PBMC). Data are expressed as the ratio between the gene of interest cell equivalent and GAPDH, yielding relative expression units (REU).

Western Blot analysis for PI3K isoforms

Naïve rats were deeply anesthetized and perfused with RT saline. Spinal cords and DRGs were removed and dissected, as above. Tissue was immediately frozen on dry ice and stored at -70°C. Protein was extracted using lysis buffer (0.5% Triton X-100, 50 mM Tris-HCl, 150

nM NaCl, 1 mM EDTA and 3% SDS) with Complete Protease Inhibitors (Roche Applied Science, Indianapolis, IN, USA). Following, determination of protein concentrations using the BCA protein assay kit (Pierce Biotechnology Inc., Rockford, IL), 30 μg protein from each sample was resolved on NuPAGE 4-12% Bis-Tris Gel (Invitrogen, Carlsbad CA, USA). After blotting on polyvinylidene membranes and blocking, blots were probed with antibodies against p110α (#4249S, Cell Signaling Technology, Danvers, MA), p110β, p110γ and p110δ (#602, #7177 and # 176, Santa Cruz Biotechnology, Santa Cruz, CA) followed by HRP-conjugated secondary antibody (Cell Signaling Technology). Antibodies against the p110 α, β and γ subunits were from rabbit, while the anti-p110δ was raised in mice. Membranes were developed using Super Signal West Femto Substrate (Pierce Biotechnology, Inc). β-actin was used as a loading control (Sigma, St. Louis, MO). Using the #7177 antibody, all Western blots for p110γ were negative using spinal cord, DRG and positive controls (data not shown), thus no conclusions could be made regarding PI3Kγ content using this technique.

Immunohistochemistry for PI3K isoform localization

Deeply anesthetized naïve rats were perfused with RT saline, followed by cold (4°C) 4% paraformaldehyde in 0.1 M phosphate buffer (PBS), pH 7.4. The lumbar enlargement, L4 and L5 DRGs and portions of the sciatic nerve were harvested and post-fixed for 6h; tissue was then cryoprotected in 30% sucrose in 0.1M PBS. Teased nerve fibers were prepared from de-sheathed uninjured sciatic nerves. Nerve bundles were separated using fine forceps and individual fibers were then teased out using 0.20-0.22 mm acupuncture needles (Vinco, Oxford Medical Supplies, UK) and dried. Fixed tissues were embedded in O.C.T. compound (Tissue-Tek, Torrance, CA, USA) and stored at -20°C. Transverse DRG and spinal cord sections (16 μm) were cut on a Leica CM 1800 cryostat. Sections were mounted and double labeled with rabbit anti PI3Kα, -β, -γ, or mouse anti PI3Kδ (1:100) and one of the following cell markers mouse anti-NeuN (neurons, 1:500; Millipore, Temecula, CA, USA), rabbit anti-OX-42 (microglia, 1:500; BioSource International, Camarillo, CA, USA), goat anti-Iba1 (microglia, 1:750, Abcam, Cambridge, MA, USA), mouse anti-glial fibrillary acidic protein (GFAP, astrocytes, 1:500; Chemicon or Sigma), rabbit anti-Olig-2 (oligodendrocytes, 1:500; Millipore), chicken anti-MAP2 (neurons, 1:500, Abcam), mouse anti-vimentin, (astrocytes 1:1000; Zymed) mouse anti-APC (oligodendrocytes, 1:500, Abcam), mouse anti-synaptophysin (neurons, 1:500, Santa Cruz), mouse anti-MBP (Schwann cells/compact myelin, 1:500, AbCam), -IB4 isolectin (nociceptive primary afferent neurons/fibers, 1:500, Invitrogen) rabbit anti-Caspr (axonal paranodes, 1:500, NeuroMab, UC Davis CA, USA) to confirm cell locations of each isoform. Binding sites were visualized with species matched goat anti-rabbit secondary antibody conjugated with Alexa Fluor 488 or goat anti-mouse antibody conjugated with Alexa Fluor 594 (both at 1:500, Invitrogen). Control sections had the primary antibody omitted and replaced with rabbit or mouse IgG, as appropriate. Images were captured with a fluorescence BX51 microscope (Olympus, Melville, NY, USA) at 10–60X. To confirm antibody co-localization, images were acquired with a Leica TCS SP5 confocal system; single optical sections of 0.3–0.4 μm thicknesses were taken and images processed with LAS AF software. All reported findings were observed in multiple sections in a minimum of 3 animals. In the instance of the teased fibers, results are representative of about 20 individual fibers.

Unilateral dorsal rhizotomies (L4-L6) were performed in some animals to determine the extent to which primary afferent fibers contributed to observed dorsal horn expression of individual kinase isoforms. Loss of dorsal horn staining after rhizotomy is indicative of primary afferent fiber localization, while residual staining is interpreted as localization in intrinsic cells and/or descending fibers. Rats were deeply anesthetized and a midline incision made over the transverse processes of L1-L3 followed by a unilateral hemilaminectomy. A small dural opening (approximately 10mm) was made and dorsal roots L4-L6 were isolated. Each rootlet was transected and a 1-2 mm segment removed. Postoperative treatment was as below. Rats displayed minimal changes in gross motor abilities and no loss of bowel or bladder function. Animals were perfused 12 days after surgery and spinal tissue processed for immunohistochemistry. One animal with incomplete denervation, as determined post mortem, was excluded.

Intrathecal (i.t.) catheterization

Following induction of isoflurane anesthesia, polyethylene (PE-5, 8.5cm, Scientific Commodities Inc, AZ) catheters were inserted caudally through an opening in the atlanto-occipital membrane to end at the rostral lumbar enlargement. All rats received subcutaneous Lactated Ringer's solution (1 cc/50g body weight, Baxter HealthCare Corporation) with carprofen (5mg/kg, Rimadyl Pfizer Inc., NY) immediately postoperatively; post-surgery, animals were housed individually. Behavioral experiments took place 5-8 days after catheterization.

Behavioral paradigm and testing

Testing was conducted between 09:00h and 16:00h. An experimenter blinded to pre-treatment substances performed all behavioral testing. Mechanical allodynia was assessed prior to drug injection (baseline) and at designated times (1, 2, 3 and 4h) after unilateral intraplantar (i.pl.) injections (hindpaw) of 2% carrageenan (100 μl, Wako Pure Chemical Industries, Ltd.). Rats were placed on an elevated mesh floor in individual test chambers. Withdrawal responses to punctate mechanical stimuli were determined using a set of 8 calibrated von Frey filaments (Stoelting, Wood Dale, IL) with buckling forces between 0.41-15.1g (4.0-148mN) as described previously [9].

Prior to carrageenan administration (2 min), freshly mixed isoform specific PI3K antagonist or the appropriate DMSO vehicle was injected i.t. (intrathecally), i.v. (intravenously) or i.pl. For i.t. administration, antagonist or vehicle (10μl) was injected through the catheter followed by a 10μl flush of isotonic sterile saline. Doses were based, in part, on our recent *in vitro* work using these agents [4] and on the relative ratio of wortmannin, required to inhibit TNF-evoked increases in P-Akt in cultured synoviocytes vs. that required to inhibit carrageenan-induced pain behavior in rats (unpublished data and [11]). The starting dose for each antagonist was determined to be 10μl of a 0.5mM solution. This resulted in initial doses of GDC-0941-2.6μg (Selleck Chemicals LLC, Houston, TX, USA), compound 15e-1.57μg (Enzo Life Sciences, Farmington, NY, USA), TGX 221-1.8μg (Cayman Chemical Company, Ann Arbor, MI., USA), Cal-101-2.1μg (Selleck Chemicals, LLC) and AS252424-1.53μg (Cayman Chemical Company). The panantagonist (GDC-0941) and the PI3Kβ antagonist (TGX 221) were also given at 1/3 and 1/9 of this starting dose. The initial

dose of each agent was dissolved in 5% DMSO/95% saline. All solutions were pH adjusted to 7.2 before use. When lower doses were employed, DMSO was diluted to 1.67% and 0.58%, respectively. In order to rule out systemic leakage and non-spinal effects of PI3K antagonists, naive rats were injected via the tail vein (100μl), using doses of GDC-0941 (2.6μg) and TGX 221 (0.6μg) that were anti-allodynic when given i.t. According to the dilution of the agent, vehicle was either 0.5 or 0.17% DMSO. Intraplantar injection of isoform specific PI3K antagonists was used to identify nociceptive effects of PI3K's at the level of the skin and peripheral nerve terminal. Antagonists (same starting dose as given i.t.) or vehicle were administered followed 2 min later by i.pl. carrageenan into the same site. This dose was given as a 50 μl volume of a 1% DMSO solution. Animals given i.v. or i.pl. antagonists had no catheters.

Subcellular membrane fractionation and Western blots

Catheterized rats were deeply anesthetized and injected i.t. with either freshly mixed PI3Kβ antagonist (1.8 μg TGX 221) or 5% DMSO, followed 2 min later by i.pl. carrageenan. Control groups were anesthetized for the same duration, but were injected with i.t. vehicle alone. Anesthesia was discontinued and rats returned to their home cages. Rats were re-anesthetized and decapitated 1h after injections. Ipsilateral lumbar dorsal spinal cords were harvested and homogenized in 4 ml hypotonic buffer. After 10 min, homogenates were centrifuged at 12,000 rcf for 10 min at 4°C and the supernatant collected. This supernatant (S1) was then centrifuged at 21,600 rcf for 30 min at 4°C and the resulting supernatant (S2) collected. S2 was centrifuged at 150,000 rpm at 4°C for 2h and the pellet washed and centrifuged again at 150,000 rcf for 2h. The resulting pellet containing plasma membranes was re-suspended in 50μl standard extraction buffer (50 mM Tris, pH 7.4; 150 mM NaCl; 1 mM EDTA, pH 8; 0.5% Triton X-100 with protease and phosphatase inhibitors) [10; 11]. GluA1 was measured in the plasma membrane fractions by Western blot. Prior to gel loading, protein concentrations were determined and gels run as before with the difference that only 15μg of protein were added to each lane. Membranes were blocked with 5% nonfat-dry milk in Tris-HCl buffer containing 0.1% Tween 20, pH 7.4 (TBS-T) for 1h at RT and then incubated at 4°C overnight, with rabbit anti-GluA1 antibody (1:1000; Millipore, Temecula, CA). Membranes were stripped and reprocessed for N-cadherin (1:1000, Cell Signalling) as loading control. Immunoblots were scanned and analyzed using ImageQuant (Amersham Biosciences, Piscataway, NJ, USA). Immunoblot density was normalized to vehicle controls run on the same gel.

Statistical Analysis

Graph Pad Prism 4.0 (GPP 4.0, GraphPad Software, Inc., San Diego, CA) was used for statistical analysis. RT-PCR and behavioral data were expressed as mean ± S.E.M. Two-way ANOVA with repeated measurements and post-hoc Bonferroni adjustment were conducted for within group comparisons of withdrawal thresholds (before and after paw injection) and time point withdrawal thresholds of rats (drug vs. vehicle). Student's t-test and ANOVA were used to compare areas under the curve (AUC) for RT-PCR and behavioral time courses. A statistical significance of $p \leq 0.05$ was accepted.

RESULTS

Expression and Distribution of PI3-K Isoforms in Spinal Cord and DRG PI3Kα

As expected, substantial amounts of mRNA for PI3Kα were detected in the spinal cord and DRG of naïve rats (Table I). Spinal cord PI3Kα levels showed a marked tendency to increase during acute inflammation, however, this increase was not significant. Although this may have been a function of the small sample size (N=3-4), levels of PI3K δ and γ respectively increased and decreased in the same tissue samples indicating a higher variability for the PI3Kα isoform. Surprisingly mRNA for PI3Kα decreased in DRGs of animals 4 h post-carrageenan injection (Table I; $p \leq 0.05$). Western blots revealed that PI3Kα protein was also present in lumbar enlargements from naïve animals (Figure 1A) as well as in DRG. In contrast to literature reports of widespread expression, spinal cord immunohistochemistry demonstrated a highly restricted cellular localization. In lumbar dorsal horn, PI3Kα was seen predominantly across the entire mediolateral extent of the superficial laminae (Figure 2A), at first glance distribution appeared to be similar to the neuronal distribution observed for PKCγ with the addition of a small amount of labeling in lamina I. However, immunoreactivity for PI3Kα did not co-localize with either of our neuronal markers (NeuN (Figure 2A and D) or MAP2 (not shown)). It also did not co-localize with GFAP, OX-42, Iba-1 or Olig2, markers for astrocytes, microglia and oligodendrocytes (data not shown). Thus, as we could not find evidence of co-localization with cell markers and much of the staining was decidedly punctate (Figure 2D), we began to look at markers for afferent terminals. Double-staining with IB4, a marker for nonpeptidergic nociceptive afferent fibers, showed some co-localization in lamina IIi (yellow), there was also strong staining in lamina III, just ventral to the IB4 positive puncta (Figure 2B) as well as a lesser scattering of positive profiles in lamina I. To determine the extent of the primary afferent contribution to the dorsal horn PI3Kα, we performed unilateral dorsal rhizotomies (L4-L6). Spinal cords of these animals exhibited a near complete ipsilateral loss of dorsal horn PI3Kα (Figure 2E), indicative of localization in central terminals of primary afferent fibers as opposed to either intrinsic dorsal horn cells or descending terminals. In ventral horn, the staining pattern for PI3Kα was totally different, with localization confined to cytosol of large neurons, and no punctate staining (Figure 2C). As in dorsal horn, no co-localization was observed with any of our glial markers (GFAP is illustrated). Following rhyzotomy, there was no change in ventral horn staining.

Presence of PI3Kα protein in DRG was confirmed by histochemistry. PI3Kα was commonly seen in neuronal somata with no apparent preference with regard to cell size (Figure 2F) or cell markers (IB4, CGRP, data not shown); it was not found within satellite cells (Figure 2G) or in individual teased primary afferent fibers (Figure 2H). Prominent DRG neuronal PI3Kα is consistent with the loss of PI3Kα in dorsal horn after rhizotomy.

PI3Kβ

Expression of PI3Kβ mRNA in spinal cord and DRG of naïve animals was easily detected (Table I). Although there was a strong trend for several hs of paw inflammation to increase PI3Kβ mRNA in the spinal cord, this did not reach significance ($p \leq 0.08$). As observed for PI3Kα, levels of PI3Kβ were concomitantly decreased in DRGs harvested 4h post

carrageenan. Presence of PI3Kβ protein in naïve spinal cord and DRGs was demonstrated by Western blot (Figure 1B). Immunohistochemistry for PI3Kβ showed widespread distribution throughout the dorsal horn (Figure 3A, C). Higher power micrographs taken from this region indicated substantial punctate staining, importantly, confocal assessment of Z-stacks in NeuN double-stained tissue showed that a significant portion of the immunoreactivity was localized to the neuronal somata, below the plasma membrane (Figure 3B). Significantly, there was a large amount of residual PI3Kβ staining in structures that did not stain with neuronal (NeuN, MAP2), astrocytic (GFAP, vimentin) or microglial (OX-42, Iba-1) markers (see supplemental Figures 1-3).

Tissue from the same rhizotomized animal shown in Figure 2E was also stained for PI3Kβ (Figure 3C). Unlike the marked asymmetrical staining pattern seen for the α isoform, PI3Kβ staining remained prominent in the dorsal horn ipsilateral to the surgery, indicating that much of the kinase was localized to intrinsic neurons or descending fibers. It must be noted that staining density in the medial dorsal horn frequently was diminished in tissue from rhyzotomized animals consistent with a contribution from central terminals of axotomized primary afferent fibers in L4-6, however this was not the case in every section. In some sections, there appeared to be an up-regulation of PI3Kβ in the dorsal root entry zone of the ipsilateral side. In naïve animals, little to no PI3Kβ staining was observed in the ventral horn (Figure 3C).

PI3Kβ in the DRG was in neurons of all sizes and appeared to be distributed throughout the cytosol (Figure 3D). When the DRGs were sectioned to include nerve fiber bundles or in dorsal rootlets that were cut prior to spinal cord entry, we observed staining for the β isoform (Figure 3D, E) in the fascicles. This contrasts to the total lack of staining for the PI3Kα in equivalent sections of nerve fibers running through the DRG (Figure 2D). In dorsal rootlets, the stained half moon shaped profiles were characteristic of Schwann cells (Figure 3F). Double staining the fiber bundles with myelin basic protein (MBP) revealed no co-localization, but rather chevron shaped PI3Kβ-stained profiles separating segments of MBP staining, consistent with PI3Kβ being in Schmidt-Lanterman incisures [27] [48]. Prominent staining in single teased fibers occurred primarily at the nodal/paranodal region (Figure 3F); otherwise there was little axonal staining along the length of the nerve fiber. Taken together, these data imply that myelinating Schwann cells are the main source of the PI3Kβ and that this isoform is potentially involved in the radial communication pathway across the myelin sheath [43]. Given the paranodal localization, it is intriguing that PI3 kinase has been implicated in up-regulation of the potassium channels Kv 1.1, 1.2 and 1.3 in HEK cells [21].

PI3Kδ

Spinal and DRG levels of PI3Kδ mRNA were detectable, but relatively low (Table I). Unlike PI3Kα and -β, there was a strong tendency towards higher levels of mRNA in DRG ($p \leq 0.064$) compared to the spinal cord. Western blots confirmed the presence of PI3Kδ protein in spinal tissue (Figure 1C). Spinal cord staining with a wide variety of cell markers did not reveal PI3Kδ in neurons, microglia or in grey matter astrocytes (data not shown). Staining was observed solely in white matter and confined to GFAP stained astrocytes with

long radial shaped processes and oligodendrocytes (Figure 4A, B). Immunohistochemical staining in DRG and nerve fibers of the naïve rat revealed no staining for PI3Kδ protein in these tissues. Lack of detectable δ isoform staining in grey matter spinal astrocytes and microglia in naïve tissue was unexpected. However as RT-PCR indicated an increase in mRNA for PI3Kδ in spinal cord harvested 4h post carrageenan ($p \leq 0.04$; Table I), it is possible that expression was up-regulated in glia at this time.

PI3Kγ

Levels of PI3Kγ mRNA in naïve dorsal spinal cord were also well within the detection limits of our assay (Table I), despite this, we were unable to detect PI3Kγ protein in spinal cord using immunocytochemistry. In DRG tissue, however, we detected mRNA for PI3Kγ and staining for the protein was seen in the soma of a subpopulation of small to medium sized, presumptive nociceptive DRG neurons (Figure 4C,D). Staining in IB4 and TRPV1 expressing DRG neurons and lack of staining in the spinal cord has previously been reported for this isoform [13; 25]. Four h post paw carrageenan, levels of PI3Kγ mRNA were seen to decrease in dorsal spinal cord ($p \leq 0.047$) and to remain stable in DRG ($p \leq 0.423$).

In summary, in naïve tissue, PI3Kβ is the only isoform found in dorsal horn neurons and no isoform is found in grey matter glia; central terminals of primary afferent fibers contain PI3Kα and -β. Four hours following carrageenan inflammation, mRNA for PI3Kδ increases in spinal cord dorsal horn. In naïve DRGs, PI3Kα and -β are found in subpopulations of neurons consisting of cells of all sizes, PI3Kγ is found selectively in a subpopulation of DRG neurons with nociceptive markers. Future immunohistochemical experiments will examine if any of these isoforms are up- or down-regulated following short term and sustained inflammation.

I.T. Antagonist Pre-treatment and Assessment of Carrageenan-induced Mechanical Allodynia

Basal mechanical paw withdrawal thresholds did not differ among the various pre-treatment groups. Following i.t. pre-treatment with 10μl DMSO, intraplantar carrageenan injection induced a steep decrease in threshold over the next 4 h (Figure 5), with the sharpest decline over the first hour. There was no difference in responses over time among groups treated with i.t. vehicle containing 0.56, 1.67 or 5.0% DMSO (2-way ANOVA). Intrathecal pre-treatment with a pan-PI3K antagonist (GDC-0941; 2.6 μg) reduced carrageenan-induced mechanical allodynia over the 4 h observation period (Figure 5A). Lower doses of this panantagonist resulted in withdrawal thresholds no different than pre-treatment with their respective DMSO vehicles.

Consistent with our observation that PI3Kβ is found in dorsal horn neurons, pretreatment with TGX 221, a selective PI3Kβ inhibitor, resulted in a dose-dependent anti-allodynic effect compared to vehicle pre-treatment. Doses of 0.6 and 1.8 μg, resulted in significant reduction in allodynia lasting at least 3 and over 4 h, respectively (Figure 5B). The lowest dose (0.2 μg), however, had no effect on behavior. Figure 5C represents integrated pain behavior over time (AUC). Both PI3K pan and -β inhibition significantly reduced carrageenan-induced pain behavior at the highest dose administered; at the mid-range dose

only selective PI3Kβ inhibition was effective. Intravenous injection of the same amount of antagonist, which was effective when administered i.t. (0.6 μg TGX221 and 2.6 μg GDC-0941), in 100 μl of DMSO vehicle was no more effective than pretreatment with vehicle alone, strongly suggesting that the i.t. effect was not due to systemic leakage (Figure 5E)

Intrathecal pre-treatment with neither Compound 15e (PI3Kα inhibitor; 1.57 μg), CAL-101 (PI3Kδ inhibitor; 2.1μg) nor AS252424 (a fairly selective PI3Kγ inhibitor with some affinity for PI3Kα; 1.53μg) was effective in blocking or reducing carrageenan-induced pain behavior at any time point (Figure 5D). Lack of effect of compound 15e was somewhat surprising in light of the strong presence of PI3Kα in nerve terminals ending in the superficial dorsal horn.

Since Class I PI3 kinases are found in peripheral neurons (DRGs), endothelial and immune cells [1; 3; 24] as well as in the spinal cord, we investigated the effect of i.pl. antagonist administration on pain behavior. Intraplantar inhibition of PI3Kβ or PI3Kγ was effective in reducing carrageenan-induced mechanical allodynia (Figure 6A). PI3Kγ antagonism (1.53 μg AS252424) resulted in a much more prominent effect, lasting for at least 2h post-injection compared to vehicle. Strikingly, thresholds were the same at 1h post carrageenan as they were at baseline. Administration of TGX221 (1.8 μg) resulted in a more modest reduction of mechanical allodynia lasting at least 1h post carrageenan injection. It is likely that the degree of anti-nociception produced by the β-antagonist was not physiological relevant. At the doses given, neither pan PI3K antagonism with GDC-0941 nor δ-(CAL-101) or α-isoform (Compound 15e) specific antagonism was effective in reducing mechanical allodynia.

AMPA Receptor Trafficking

As reported in our previous studies [10; 11], intraplantar carrageenan induces an approximately 3-fold increase in the level of GluA1 in plasma membrane fractions of ipsilateral dorsal spinal cord from vehicle pre-treated animals (Figure 7). Pre-treatment with the PI3Kβ specific antagonist completely blocked this increase. Blockade of carrageenan-induced GluA1 subunit trafficking to the membrane in dorsal spinal cord has been observed previously following i.t. pretreatment with LY294002, a non-selective PI3K antagonist (unpublished data).

In summary, PI3Kβ is the only PI3K isoform found in intrinsic dorsal horn neurons in naïve animals. Intrathecal administration of only the PI3Kβ selective antagonist blocked paw carrageenan induced pain behavior and trafficking of dorsal horn GluA1 AMPA receptor subunits into plasma membranes. The PI3Kγ isoform is exclusively found in nociceptive afferent fibers and its intraplantar antagonism is the most effective in blocking carrageenan-induced pain behavior.

Discussion

The data show that all four Class I PI3K isoforms are differentially located in spinal cord, DRG and peripheral nerve in naïve animals and that the -β and -γ isoforms have unique roles

in mediating nociception resulting from acute peripheral inflammation. Intrathecal or intraplantar pre-treatment with nonselective PI3K antagonists, such as wortmannin and LY294002, dose dependently reduce pain behavior induced by peripheral injection of nociceptive chemical stimuli [34] [11; 46; 52; 55]. We refine these previous findings to show that selective spinal PI3Kβ inhibition is sufficient to block carrageenan-induced allodynia, while specific antagonism of the other Class I PI3K isoforms is ineffective. Increased anti-allodynia produced by equimolar doses of TGX-221 compared to the pan antagonist is explained by its higher IC_{50} for the β isoform.

This specific role played by PI3Kβ in spinal sensitization is substantiated by the discovery that in naïve spinal cord, only the PI3Kβ isoform is found in dorsal horn neurons and that its antagonism blocks inflammation-induced spinal AMPA trafficking to the membrane. In hippocampus, PI3K can cross-link with AMPAr subunit complexes resulting in increased rates of GluA1 insertion into neuronal plasma membranes [26; 36]. We have recently shown that TNF-induced insertion of Ca^{2+} -permeable AMPAr into both dorsal horn neurons and motor neurons is blocked by pre-incubation with wortmannin, a non-selective PI3K antagonist [51; 53]. Activity induced AMPA receptor trafficking is thought to contribute, in great part, to excitotoxic loss of motor neurons following spinal injury [19] and to allodynia and hyperalgesia in dorsal horn sensory neurons [11; 20; 32].

Surprisingly, none of the Class I PI3K isoforms including PI3Kδ nor -γ were seen in glia within spinal cord grey matter. However, i.t. injection of more than three times as much of the γ antagonist as used in this study elicited no change in either trypsin-induced nociception or pruritis [33], supporting the lack of spinal PI3Kγ staining and the negative behavioral results with i.t. injection that we observed. One limitation of our study is that our data only examines naïve tissue and acute inflammation. Protein levels of some of the PI3K isoforms increase during chronic inflammation or following an ischemia-reperfusion paradigm [41], this is in agreement with out observations in the spinal cord where spinal mRNA for PI3Kδ is increased 4 h after induction of inflammation. In addition we observed a strong tendency for mRNA for PI3K α and -β to increase at this same time. Some of the injury-induced, newly expressed PI3K could conceivably be expressed in spinal glia or in other previously unidentified cell types including infiltrating immune cells. In this regard, our focus on naïve tissue and acute inflammation could be considered to be too restrictive. Thus, future experiments will address cellular localization of PI3K isoforms and the ability of the antagonists to block nociception in animals during later stages of inflammation. Accordingly, we have started using histochemistry to look for PI3K isoforms in spinal cords harvested from rats 4h after paw carrageenan injection. Preliminary results indicate that at this timepoint, PI3Kδ is found in a small population of GFAP staining processes, presumably astrocytes, in grey matter of the superficial dorsal horn whereas previously it was only observed in white matter.

Preliminary results indicate that at this timepoint, PI3Kδ is found in a small population of GFAP staining processes, presumably astrocytes, in grey matter of the superficial dorsal horn.

Similar to results published by others [3], protein for the α, β and γ, but not δ, PI3K isoforms was identified in naïve ganglia. These investigators also reported that mRNA for all four PI3K isoforms is present in the DRG and trigeminal ganglia. More recently, PI3Kγ has been identified in small to medium size neurons, which double stained for IB4 or TRPV1 [13; 25]. Interestingly, PI3Kδ has been reported in the ventral horn and peripheral nervous system of E13.5 mice and PI3Kδ knock out mice display reduced nerve regeneration post injury [18], this raises the possibility that different isoforms are expressed during development and under conditions of regeneration or extreme physiological stress.

Although, PI3Ks have important roles in Schwann cells and contribute to myelination in Schwann cell-DRG co-cultures[30] [8], [28], our work is the first to imply that the most relevant isoform for Schwann cells is PI3Kβ. Localization of this isoform to the paranodal region of nerve fibers is also a novel finding. Despite these specific peripheral PI3Kβ-containing sites, i.pl. pre-treatment with the PI3Kβ antagonist resulted in only a transient blockade of carrageenan induced allodynia at 1h. Similar i.pl. antagonism of the γ-isoform resulted in a more profound and prolonged anti-allodynic effect. These data conflict with those of Ferreira and colleagues [13; 14] who found that morphine's peripheral anti-hyperalgesia actions are dependent on intact PI3Kγ in the paw. This discrepancy might, in part, be attributed to many differences in protocols, because the two studies used different antagonists with different relative γ/α selectivities, however, Ferreira's group observed a similar loss of morphine efficacy following the use of PI3Kγ antisense, which strengthens their observation. Importantly, several other groups have demonstrated that peripheral inflammation results in selective phosphorylation of AKT in small to medium TRPV1/IB4 staining DRG neurons [46; 47; 55], similar to the PI3Kγ containing population. Nonselective PI3K or AKT antagonism in these animals significantly reduces pain behavior [11; 35].

Importantly, i.pl. injection of carrageenan elicits nociception by more than just direct neuronal sensitization. Inflammatory mediators, such as TNF, both elicit a PI3Kα/AKT dependent decrease in vascular endothelial junctional integrity and act as chemotactic agents. Consequently, increased levels of these agents co-varies with increase migration of neutrophils [6; 7]. Given that i.pl. carrageenan [12], also induces TNF release in the paw and infiltration of immune cells [37; 38], it is reasonable to hypothesize that some of the antinociceptive effects of the i.pl. PI3K antagonists might be indirect via control of inflammation. Indeed, blockade of neutrophil adhesion dose dependently reduces carrageenan induced mechanical hyperalgesia [15].

In summary, the cellular distribution of all four Class I PI3K isoforms is highly regulated within the naïve spinal cord and peripheral nervous system. In spinal dorsal horn, PI3Kβ is the only isoform found in neurons, where it participates in carrageenan-induced pain behavior and AMPA receptor trafficking. This isoform is also enriched within the Schwann cell Schmidt-Lanterman incisures and the paranodes. Thus, it may also play a role in Schwann cell to axonal communication. In DRG, distribution of only the γ isoform is limited to nociceptive neurons and intraplantar injection of its antagonist profoundly reduces pain behavior. Thus, different isoforms likely participate in nociception due to inflammation via different mechanisms at varying sites. While it is possible that intrathecal PI3Kβ

antagonism might have therapeutic benefits, a peripherally acting PI3Kγ antagonist-containing agent may have a better side effect profile. Development of such agents for the treatment of inflammatory diseases is currently underway.

Supplementary Material

Refer to Web version on PubMed Central for supplementary material.

Acknowledgments

Supported by The National Institutes of Health NS 67459 (LSS), AI 070555 (GSF) and National Honor Scientist Program, in Korea (BKK)

We would like to thank Drs. Gary Bennett and Tony Yaksh for reading earlier versions of the manuscript and Dr. Mike Vasko for helpful discussions. We would like to thank Ms Joanne Steinauer for expert technical assistance.

BIBLIOGRAPHY

1. Ali K, Camps M, Pearce WP, Ji H, Ruckle T, Kuehn N, Pasquali C, Chabert C, Rommel C, Vanhaesebroeck B. Isoform-specific functions of phosphoinositide 3-kinases: p110 delta but not p110 gamma promotes optimal allergic responses in vivo. Journal of immunology. 2008; 180(4): 2538–2544.
2. Arbuckle MI, Komiyama NH, Delaney A, Coba M, Garry EM, Rosie R, Allchorne AJ, Forsyth LH, Bence M, Carlisle HJ, O'Dell TJ, Mitchell R, Fleetwood-Walker SM, Grant SG. The SH3 domain of postsynaptic density 95 mediates inflammatory pain through phosphatidylinositol-3-kinase recruitment. EMBO Rep. 2010; 11(6):473–478. [PubMed: 20467438]
3. Bartlett SE, Reynolds AJ, Tan T, Heydon K, Hendry IA. Differential mRNA expression and subcellular locations of PI3-kinase isoforms in sympathetic and sensory neurons. Journal of neuroscience research. 1999; 56(1):44–53. [PubMed: 10213474]
4. Bartok B, Boyle DL, Liu Y, Ren P, Ball ST, Bugbee WD, Rommel C, Firestein GS. PI3 Kinase delta Is a Key Regulator of Synoviocyte Function in Rheumatoid Arthritis. The American journal of pathology. 2012
5. Boyle DL, Rosengren S, Bugbee W, Kavanaugh A, Firestein GS. Quantitative biomarker analysis of synovial gene expression by real-time PCR. Arthritis research & therapy. 2003; 5(6):R352–360. [PubMed: 14680510]
6. Cain RJ, Vanhaesebroeck B, Ridley AJ. The PI3K p110alpha isoform regulates endothelial adherens junctions via Pyk2 and Rac1. J Cell Biol. 2010; 188(6):863–876. [PubMed: 20308428]
7. Cain RJ, Vanhaesebroeck B, Ridley AJ. Different PI 3-kinase inhibitors have distinct effects on endothelial permeability and leukocyte transmigration. Int J Biochem Cell Biol. 2012; 44(11):1929–1936. [PubMed: 22814170]
8. Campana WM, Hiraiwa M, O'Brien JS. Prosaptide activates the MAPK pathway by a G-protein-dependent mechanism essential for enhanced sulfatide synthesis by Schwann cells. Faseb J. 1998; 12(3):307–314. [PubMed: 9506474]
9. Chaplan SR, Bach FW, Pogrel JW, Chung JM, Yaksh TL. Quantitative assessment of tactile allodynia in the rat paw. Journal of Neuroscience Methods. 1994; 53(1):55–63. [PubMed: 7990513]
10. Choi JI, Koehrn FJ, Sorkin LS. Carrageenan induced phosphorylation of Akt is dependent on neurokinin-1 expressing neurons in the superficial dorsal horn. Molecular pain. 2012; 8:4. [PubMed: 22243518]
11. Choi JI, Svensson CI, Koehrn FJ, Bhuskute A, Sorkin LS. Peripheral inflammation induces tumor necrosis factor dependent AMPA receptor trafficking and Akt phosphorylation in spinal cord in addition to pain behavior. Pain. 2010; 149(2):243–253. [PubMed: 20202754]
12. Cunha FQ, Poole S, Lorenzetti BB, Ferreira SH. The pivotal role of tumour necrosis factor alpha in the development of inflammatory hyperalgesia. British Journal of Pharmacology. 1992; 107(3): 660–664. [PubMed: 1472964]

13. Cunha TM, Roman-Campos D, Lotufo CM, Duarte HL, Souza GR, Verri WA Jr, Funez MI, Dias QM, Schivo IR, Domingues AC, Sachs D, Chiavegatto S, Teixeira MM, Hothersall JS, Cruz JS, Cunha FQ, Ferreira SH. Morphine peripheral analgesia depends on activation of the PI3Kgamma/AKT/nNOS/NO/KATP signaling pathway. Proceedings of the National Academy of Sciences of the United States of America. 2010; 107(9):4442–4447. [PubMed: 20147620]

14. Cunha TM, Souza GR, Domingues AC, Carreira EU, Lotufo CM, Funez MI, Verri WA Jr, Cunha FQ, Ferreira SH. Stimulation of peripheral kappa opioid receptors inhibits inflammatory hyperalgesia via activation of the PI3Kgamma/AKT/nNOS/NO signaling pathway. Molecular pain. 2012; 8:10. [PubMed: 22316281]

15. Cunha TM, Verri WA Jr, Schivo IR, Napimoga MH, Parada CA, Poole S, Teixeira MM, Ferreira SH, Cunha FQ. Crucial role of neutrophils in the development of mechanical inflammatory hypernociception. Journal of leukocyte biology. 2008; 83(4):824–832. [PubMed: 18203872]

16. Dagia NM, Agarwal G, Kamath DV, Chetrapal-Kunwar A, Gupte RD, Jadhav MG, Dadarkar SS, Trivedi J, Kulkarni-Almeida AA, Kharas F, Fonseca LC, Kumar S, Bhonde MR. A preferential p110alpha/gamma PI3K inhibitor attenuates experimental inflammation by suppressing the production of proinflammatory mediators in a NF-kappaB-dependent manner. Am J Physiol Cell Physiol. 2010; 298(4):C929–941. [PubMed: 20089935]

17. Duan B, Liu DS, Huang Y, Zeng WZ, Wang X, Yu H, Zhu MX, Chen ZY, Xu TL. PI3-kinase/Akt pathway-regulated membrane insertion of acid-sensing ion channel 1a underlies BDNF-induced pain hypersensitivity. The Journal of neuroscience : the official journal of the Society for Neuroscience. 2012; 32(18):6351–6363. [PubMed: 22553040]

18. Eickholt BJ, Ahmed AI, Davies M, Papakonstanti EA, Pearce W, Starkey ML, Bilancio A, Need AC, Smith AJ, Hall SM, Hamers FP, Giese KP, Bradbury EJ, Vanhaesebroeck B. Control of axonal growth and regeneration of sensory neurons by the p110delta PI 3-kinase. PLoS One. 2007; 2(9):e869. [PubMed: 17846664]

19. Ferguson AR, Christensen RN, Gensel JC, Miller BA, Sun F, Beattie EC, Bresnahan JC, Beattie MS. Cell death after spinal cord injury is exacerbated by rapid TNF alpha-induced trafficking of GluR2-lacking AMPARs to the plasma membrane. J Neurosci. 2008; 28(44):11391–11400. [PubMed: 18971481]

20. Galan A, Laird JM, Cervero F. In vivo recruitment by painful stimuli of AMPA receptor subunits to the plasma membrane of spinal cord neurons. Pain. 2004; 112(3):315–323. [PubMed: 15561387]

21. Gamper N, Fillon S, Huber SM, Feng Y, Kobayashi T, Cohen P, Lang F. IGF-1 up-regulates K+ channels via PI3-kinase, PDK1 and SGK1. Pflugers Arch. 2002; 443(4):625–634. [PubMed: 11907830]

22. Hawkins PT, Anderson KE, Davidson K, Stephens LR. Signalling through Class I PI3Ks in mammalian cells. Biochem Soc Trans. 2006; 34(Pt 5):647–662. [PubMed: 17052169]

23. Hirsch E, Ciraolo E, Ghigo A, Costa C. Taming the PI3K team to hold inflammation and cancer at bay. Pharmacology & therapeutics. 2008; 118(2):192–205. [PubMed: 18420279]

24. Hirsch E, Katanaev VL, Garlanda C, Azzolino O, Pirola L, Silengo L, Sozzani S, Mantovani A, Altruda F, Wymann MP. Central role for G protein-coupled phosphoinositide 3-kinase gamma in inflammation. Science. 2000; 287(5455):1049–1053. [PubMed: 10669418]

25. Konig C, Gavrilova-Ruch O, von Banchet GS, Bauer R, Grun M, Hirsch E, Rubio I, Schulz S, Heinemann SH, Schaible HG, Wetzker R. Modulation of mu opioid receptor desensitization in peripheral sensory neurons by phosphoinositide 3-kinase gamma. Neuroscience. 2010; 169(1): 449–454. [PubMed: 20451587]

26. Lee HK, Takamiya K, Han JS, Man H, Kim CH, Rumbaugh G, Yu S, Ding L, He C, Petralia RS, Wenthold RJ, Gallagher M, Huganir RL. Phosphorylation of the AMPA receptor GluR1 subunit is required for synaptic plasticity and retention of spatial memory. Cell. 2003; 112(5):631–643. [PubMed: 12628184]

27. Martini R, Schachner M. Immunoelectron microscopic localization of neural cell adhesion molecules (L1, N-CAM, and MAG) and their shared carbohydrate epitope and myelin basic protein in developing sciatic nerve. J Cell Biol. 1986; 103(6 Pt 1):2439–2448. [PubMed: 2430983]

28. Monje PV, Bartlett Bunge M, Wood PM. Cyclic AMP synergistically enhances neuregulin-dependent ERK and Akt activation and cell cycle progression in Schwann cells. Glia. 2006; 53(6): 649–659. [PubMed: 16470843]
29. Morello F, Perino A, Hirsch E. Phosphoinositide 3-kinase signalling in the vascular system. Cardiovasc Res. 2009; 82(2):261–271. [PubMed: 19038971]
30. Ogata T, Iijima S, Hoshikawa S, Miura T, Yamamoto S, Oda H, Nakamura K, Tanaka S. Opposing extracellular signal-regulated kinase and Akt pathways control Schwann cell myelination. The Journal of neuroscience : the official journal of the Society for Neuroscience. 2004; 24(30):6724–6732. [PubMed: 15282275]
31. Okkenhaug K, Vanhaesebroeck B. PI3K in lymphocyte development, differentiation and activation. Nat Rev Immunol. 2003; 3(4):317–330. [PubMed: 12669022]
32. Park JS, Yaster M, Guan X, Xu JT, Shih MH, Guan Y, Raja SN, Tao YX. Role of spinal cord alpha-amino-3-hydroxy-5-methyl-4-isoxazolepropionic acid receptors in complete Freund's adjuvant-induced inflammatory pain. Mol Pain. 2008; 4:67. [PubMed: 19116032]
33. Pereira PJ, Lazarotto LF, Leal PC, Lopes TG, Morrone FB, Campos MM. Inhibition of phosphatidylinositol-3 kinase gamma reduces pruriceptive, inflammatory, and nociceptive responses induced by trypsin in mice. Pain. 2011; 152(12):2861–2869. [PubMed: 22001656]
34. Pezet S, Marchand F, D'Mello R, Grist J, Clark AK, Malcangio M, Dickenson AH, Williams RJ, McMahon SB. Phosphatidylinositol 3-kinase is a key mediator of central sensitization in painful inflammatory conditions. J Neurosci. 2008; 28(16):4261–4270. [PubMed: 18417706]
35. Pezet S, Spyropoulos A, Williams RJ, McMahon SB. Activity-dependent phosphorylation of Akt/PKB in adult DRG neurons. Eur J Neurosci. 2005; 21(7):1785–1797. [PubMed: 15869474]
36. Pincheira R, Castro AF, Ozes ON, Idumalla PS, Donner DB. Type 1 TNF receptor forms a complex with and uses Jak2 and c-Src to selectively engage signaling pathways that regulate transcription factor activity. J Immunol. 2008; 181(2):1288–1298. [PubMed: 18606683]
37. Puri KD, Doggett TA, Douangpanya J, Hou Y, Tino WT, Wilson T, Graf T, Clayton E, Turner M, Hayflick JS, Diacovo TG. Mechanisms and implications of phosphoinositide 3-kinase delta in promoting neutrophil trafficking into inflamed tissue. Blood. 2004; 103(9):3448–3456. [PubMed: 14751923]
38. Puri KD, Doggett TA, Huang CY, Douangpanya J, Hayflick JS, Turner M, Penninger J, Diacovo TG. The role of endothelial PI3Kgamma activity in neutrophil trafficking. Blood. 2005; 106(1): 150–157. [PubMed: 15769890]
39. Rommel C, Camps M, Ji H. PI3K delta and PI3K gamma: partners in crime in inflammation in rheumatoid arthritis and beyond? Nat Rev Immunol. 2007; 7(3):191–201. [PubMed: 17290298]
40. Ruckle T, Schwarz MK, Rommel C. PI3Kgamma inhibition: towards an 'aspirin of the 21st century'? Nat Rev Drug Discov. 2006; 5(11):903–918. [PubMed: 17080027]
41. Sakurai M, Hayashi T, Abe K, Itoyuama Y, Tabayashi K. Induction of phosphatidylinositol 3-kinase and serine-threonine kinase-like immunoreactivity in rabbit spinal cord after transient ischemia. Neuroscience letters. 2001; 302(1):17–20. [PubMed: 11278101]
42. Sasaki T, Irie-Sasaki J, Jones RG, Oliveira-dos-Santos AJ, Stanford WL, Bolon B, Wakeham A, Itie A, Bouchard D, Kozieradzki I, Joza N, Mak TW, Ohashi PS, Suzuki A, Penninger JM. Function of PI3Kgamma in thymocyte development, T cell activation, and neutrophil migration. Science. 2000; 287(5455):1040–1046. [PubMed: 10669416]
43. Scherer SS. Nodes, paranodes, and incisures: from form to function. Annals of the New York Academy of Sciences. 1999; 883:131–142. [PubMed: 10586239]
44. Stein AT, Ufret-Vincenty CA, Hua L, Santana LF, Gordon SE. Phosphoinositide 3-kinase binds to TRPV1 and mediates NGF-stimulated TRPV1 trafficking to the plasma membrane. J Gen Physiol. 2006; 128(5):509–522. [PubMed: 17074976]
45. Stellwagen D, Beattie EC, Seo JY, Malenka RC. Differential regulation of AMPA receptor and GABA receptor trafficking by tumor necrosis factoralpha. J Neurosci. 2005; 25(12):3219–3228. [PubMed: 15788779]
46. Sun R, Yan J, Willis WD. Activation of protein kinase B/Akt in the periphery contributes to pain behavior induced by capsaicin in rats. Neuroscience. 2007; 144(1):286–294. [PubMed: 17084039]

47. Sun RQ, Tu YJ, Yan JY, Willis WD. Activation of protein kinase B/Akt signaling pathway contributes to mechanical hypersensitivity induced by capsaicin. Pain. 2006; 120(1-2):86–96. [PubMed: 16360265]
48. Tricaud N, Perrin-Tricaud C, Bruses JL, Rutishauser U. Adherens junctions in myelinating Schwann cells stabilize Schmidt-Lanterman incisures via recruitment of p120 catenin to E-cadherin. The Journal of neuroscience : the official journal of the Society for Neuroscience. 2005; 25(13):3259–3269. [PubMed: 15800180]
49. Viard P, Butcher AJ, Halet G, Davies A, Nurnberg B, Heblich F, Dolphin AC. PI3K promotes voltage-dependent calcium channel trafficking to the plasma membrane. Nature neuroscience. 2004; 7(9):939–946.
50. Wetzker R, Rommel C. Phosphoinositide 3-kinases as targets for therapeutic intervention. Curr Pharm Des. 2004; 10(16):1915–1922. [PubMed: 15180528]
51. Wigerblad G, Koehrn FJ, Yin HZ, Weiss JH, Svensson CI, Sorkin LS. Spinal TNF-driven neuronal trafficking of GluA1 is dependent on PI3K and PKA activity in inflammatory pain. Neurosci Abs. 2012 #429.406.
52. Xu Q, Fitzsimmons B, Steinauer J, Neill AO, Newton AC, Hua XY, Yaksh TL. Spinal phosphinositide 3-kinase-Akt-mammalian target of rapamycin signaling cascades in inflammation-induced hyperalgesia. J Neurosci. 2011; 31(6):2113–2124. [PubMed: 21307248]
53. Yin HZ, Hsu C-I, Yu S, Rao SD, Koehrn FJ, Sorkin LS, Weiss JH. TNF- α alpha triggers rapid membrane insertion of Ca2+ AMPA channels into adult MNs and enhances slow MN injury caused by glutamate transport inhibition in orgaontypic spinal cord slice cultures. Experimental Neurology. 2012
54. York RD, Molliver DC, Grewal SS, Stenberg PE, McCleskey EW, Stork PJ. Role of phosphoinositide 3-kinase and endocytosis in nerve growth factorinduced extracellular signal-regulated kinase activation via Ras and Rap1. Mol Cell Biol. 2000; 20(21):8069–8083. [PubMed: 11027277]
55. Zhuang ZY, Xu H, Clapham DE, Ji RR. Phosphatidylinositol 3-kinase activates ERK in primary sensory neurons and mediates inflammatory heat hyperalgesia through TRPV1 sensitization. The Journal of neuroscience : the official journal of the Society for Neuroscience. 2004; 24(38):8300–8309. [PubMed: 15385613]

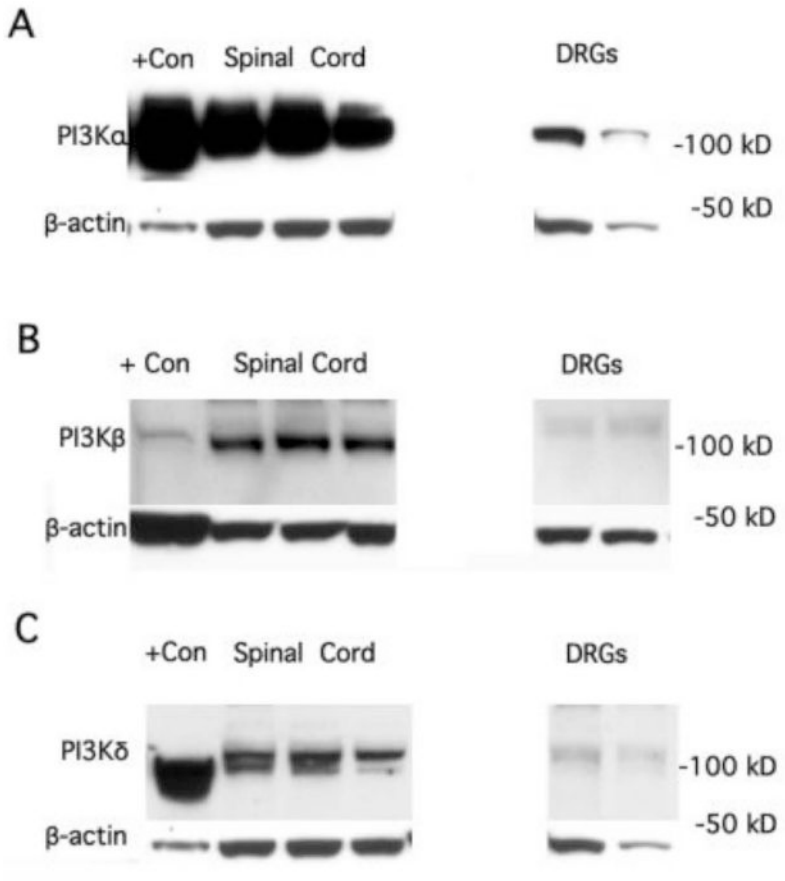

Figure 1.

A. Western blots indicating presence of PI3Kα protein in rat spinal cord and DRGs. RAW cells (derived from a macrophage-like cell line) known to contain this isoform were run as a positive (+) control. Each spinal cord or DRG blot is from a different animal. B. Western blots indicate presence of PI3Kβ protein in rat lumbar spinal cord as well as DRGs. Rat PBMCs were used as an internal positive control. C. Western blots indicate the presence of PI3Kδ protein in spinal cord. The signal from DRG was comparatively weak. RAW cells known to contain this isoform were run as a positive control. Beta-actin was used as a loading control for all isoforms.

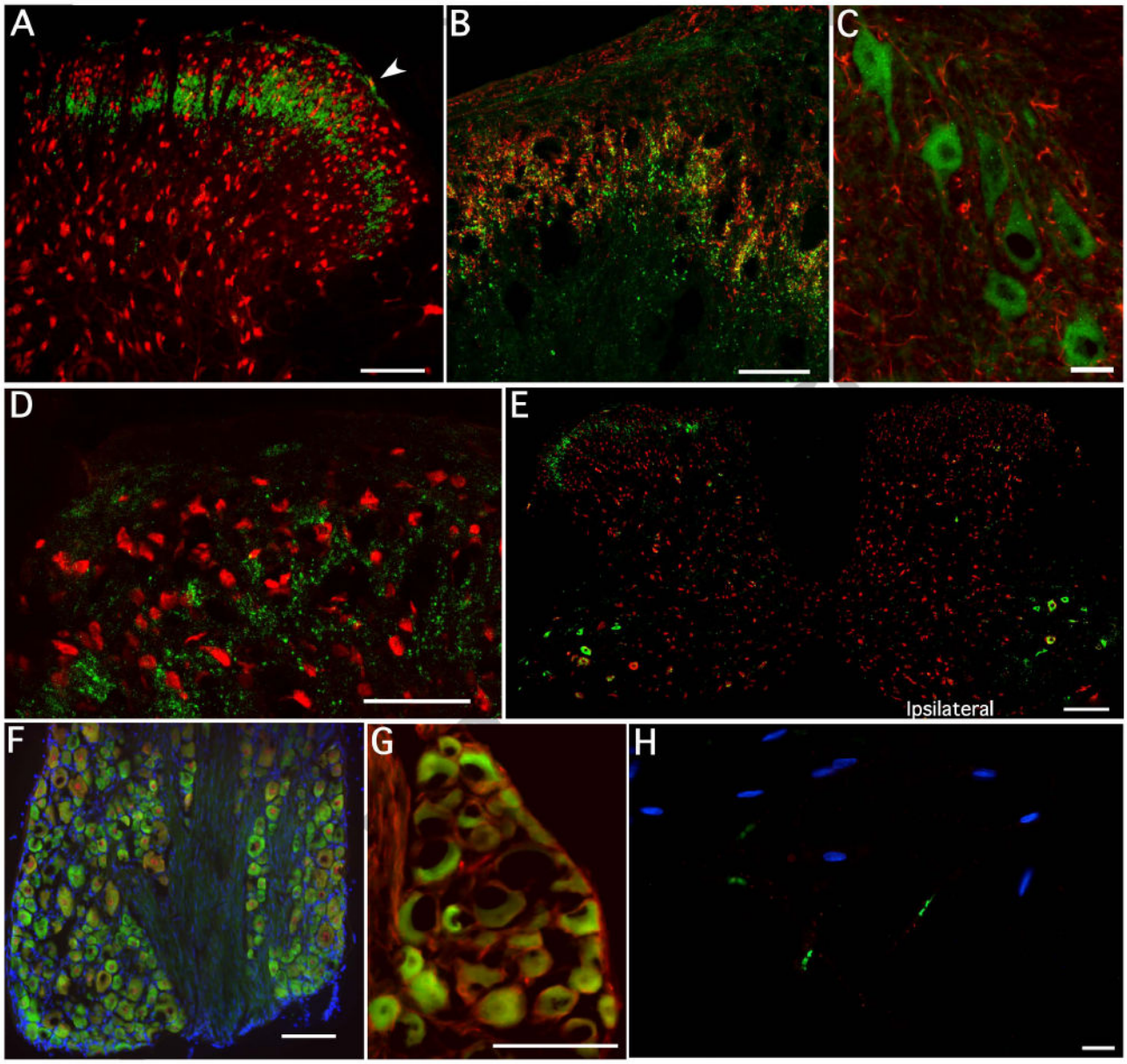

Figure 2.

Staining for PI3Kα in spinal cord, DRG and nerve. A. Representative transverse micrograph of naïve lumbar spinal cord labeled for PI3Kα (green) and NeuN (red). The PI3Kα appears to stain predominantly in an arch across the substantia gelatinosa although there is clearly also some staining in lamina I (arrowhead). Occasional staining was also seen as spots in deeper laminae, but this was infrequent and is not illustrated in this section. B). At higher power, most of the PI3Kα in dorsal horn appears to be at the same level as, and slightly more ventral to IB4 staining (red). Importantly, staining appears to be punctate, and although there is some co-localization with IB4, the majority of staining does not appear to overlap and is deeper in lamina III. C). Ventral horn double stained for PI3Kα (green) and GFAP (red) displays no co-localization with astrocytes or microglia (data not shown). D). Higher power micrograph of dorsal horn with NeuN (red) and punctate Pi3Kα (green)

staining show no overlap, but illustrates a pattern of large, frequently intersecting circles for the kinase E). Following a unilateral dorsal root rhizotomy, staining for PI3Kα (green) disappears in the dorsal horn ipsilateral to the lesion, but importantly remains in the contralateral dorsal horn. F) In naïve L4-5 DRG, PI3Kα (green) appears to be expressed in neurons of all sizes (NeuN shown in red, DAPI in blue), clearly all neurons do not express PI3Kα. Importantly, there is no PI3Kα staining in the fiber tracts separating the populations of neurons. G) High power micrograph of DRG confirms the presence of PI3Kα in neurons, but indicates no co-staining with GFAP (red), indicative of a lack of staining in non-activated satellite cells. PI3Kα frequently stains throughout the cytoplasm, but it is totally absent in the nuclei. H). Single teased sciatic nerve fibers stained for DAPI (blue), Caspr (green) and PI3Kα (red). No PI3Kα staining was observed. Size markers for panels A, F and G= 100μm, B and D= 50μm, E= 250μm and C and H= 25μm.

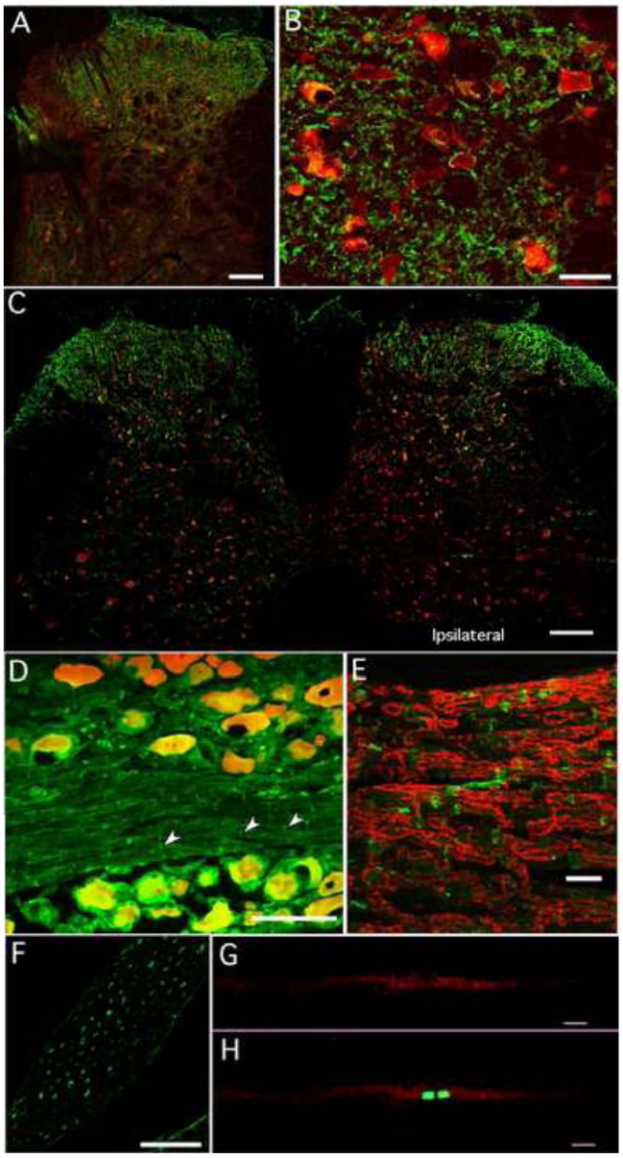

Figure 3.

Staining for PI3Kβ in spinal cord, DRG and nerve. A). Representative transverse photomicrograph labeled with PI3Kβ (green) and NeuN (red). PI3Kβ expression is more widespread throughout the dorsal horn than observed for PI3Kα. B). At higher power PI3Kβ appears to be under the neuronal plasma membrane in a thin cytoplasmic layer. C). Tissue section in close proximity to that shown in Figure 2E, illustrates that after dorsal root rhizotomy significant PI3Kβ remains in the ipsilateral side indicating that much of the dorsal horn PI3Kβ is not derived from primary afferent fibers. D). In naïve DRG, PI3Kβ (green) appears to be expressed in a subpopulation of neurons (red; double staining shown in yellow) with no specificity regarding size. There was also PI3Kβ staining in small vertical lines (arrow heads) within the fiber tracks. E) A higher-powered micrograph of a fiber tract in tissue co-stained for myelin basic protein (MBP, red) showed no double staining indicating that the PI3Kβ was not localized to compact myelin. Rather it seemed to separate

short stretches of MBP, frequently the PI3Kβ-stained profile was wedge-shaped. F). Cross sections of dorsal rootlets just prior to dorsal horn entry also revealed PI3Kβ staining. Many of the profiles were donut or half-moon shaped, suggestive of Schwann cells. G. Panel illustrates clusters of PI3Kβ positive puncta along the length of a single teased sciatic nerve fiber. H. The same nerve fiber shown in G double stained for Caspr (green) indicates that PI3Kβ is found at the paranodal region of the axons. Size markers for panels A and D= 100μm, B= 25μm, C= 250μm, E=20μm, F= 50μm and G and H= 10μm.

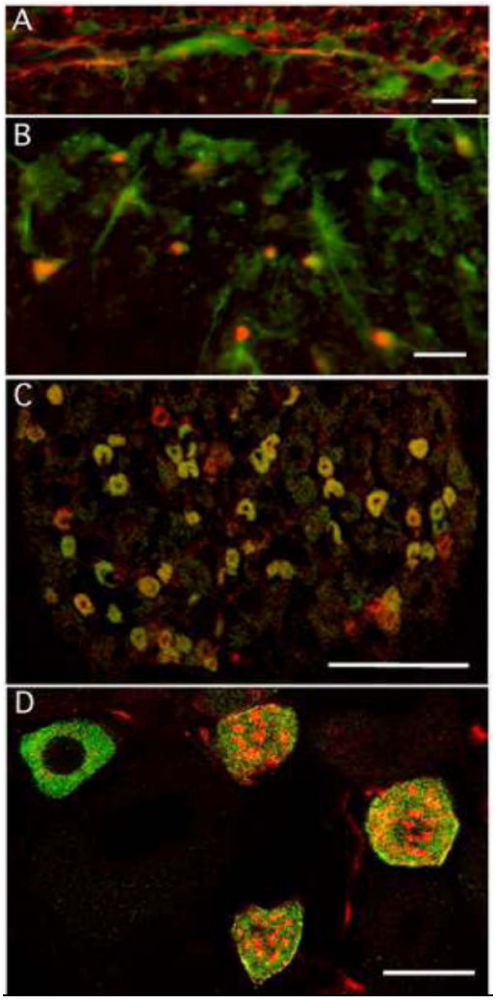

Figure 4.

Staining for PI3Kδ in spinal cord (A,B). Panel A illustrates double staining for GFAP (red) and PI3Kδ (green) in naïve spinal cord. The PI3K associated with GFAP only in white and not in grey matter. Astrocytes thus identified all ran radially from the spinal cord surface towards either the dorsal or ventral horns. Panel B shows double staining with PI3Kδ and the oligodendrocyte marker, Olig2 (red), again this was observed only in white matter. Unlike the astrocytes, PI3K staining in the oligodendrocytes was seen selectively in the peripheral processes rather than the cell body. C. In DRG, PI3Kγ-like staining was observed predominantly in cell bodies of small to medium sized neurons with nociceptive markers such as IB4 (red). Colocalization indicated in yellow. D. Higher magnification picture of individual DRG neurons indicates that the PI3Kγ appeared to be uniformly dispersed throughout the cytosol. Size markers for panels A and B= 20μm, panel C = 200μm and D= 25μm.

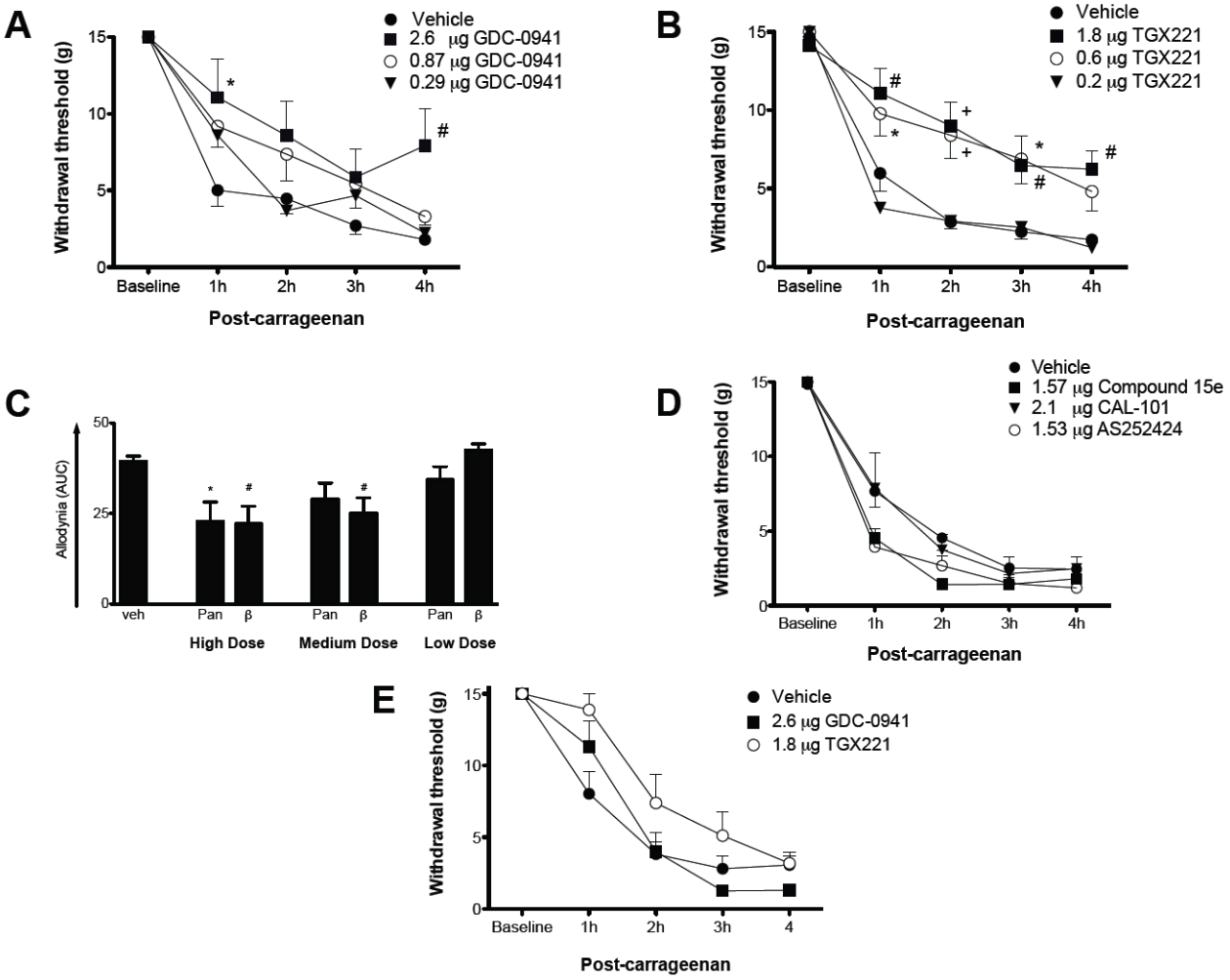

Figure 5.

Only one PI3K isoform selective antagonist reduced paw carrageenan-induced allodynia when given i.t. A). Intrathecal pre-treatment with GDC-0941, a pan-PI3K antagonist, dose dependently reduced allodynia measured over the 4h after carrageenan. B). Intrathecal pre-treatment with a selective PI3Kβ antagonist, TGX 221 also elicited a dose dependent anti-allodynia over the entire test period. C). Assessment of area under the curve confirmed anti-allodynia for the high dose of both the pan- and β isoform-specific PI3K antagonists and the medium dose of the β isoform-specific PI3K antagonist only. D). Intrathecal pretreatment with antagonists to the other three Class I PI3K isoforms was without effect. E). The same doses of the pan- and β isoform-specific PI3K antagonists that were anti-allodynic when given i.t., failed to block paw carrageenan induced allodynia when administered i.v. 1-way and 2-way ANOVA comparisons with post-hoc Bonferroni corrections; *$P < 0.05$, #$P < 0.01$, +$P < 0.001$.

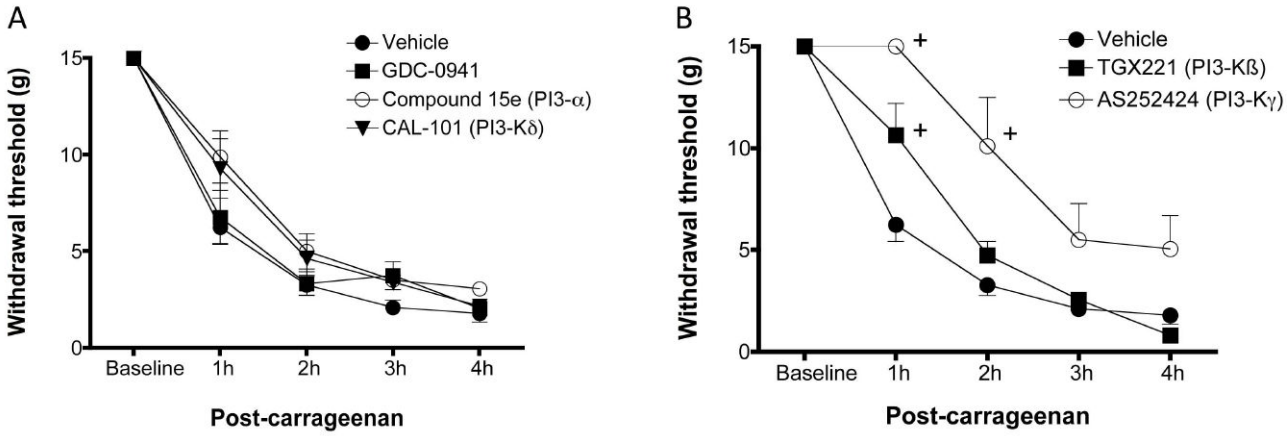

Figure 6.

Effects of intraplantar antagonism. A). Unlike i.t. pretreatment, intraplantar pretreatment with the PI3Kβ antagonist resulted in only a minor decrease in allodynia within the first hour. However, i.pl. pre-treatment with the PI3Kγ antagonist resulted in profound blockade of carrageenan-induced allodynia. B). Administration of the pan-, α or δ isoform specific antagonist at these doses was without any major effect. 2-way ANOVA comparisons with post-hoc Bonferroni corrections; + P≤ 0.01.

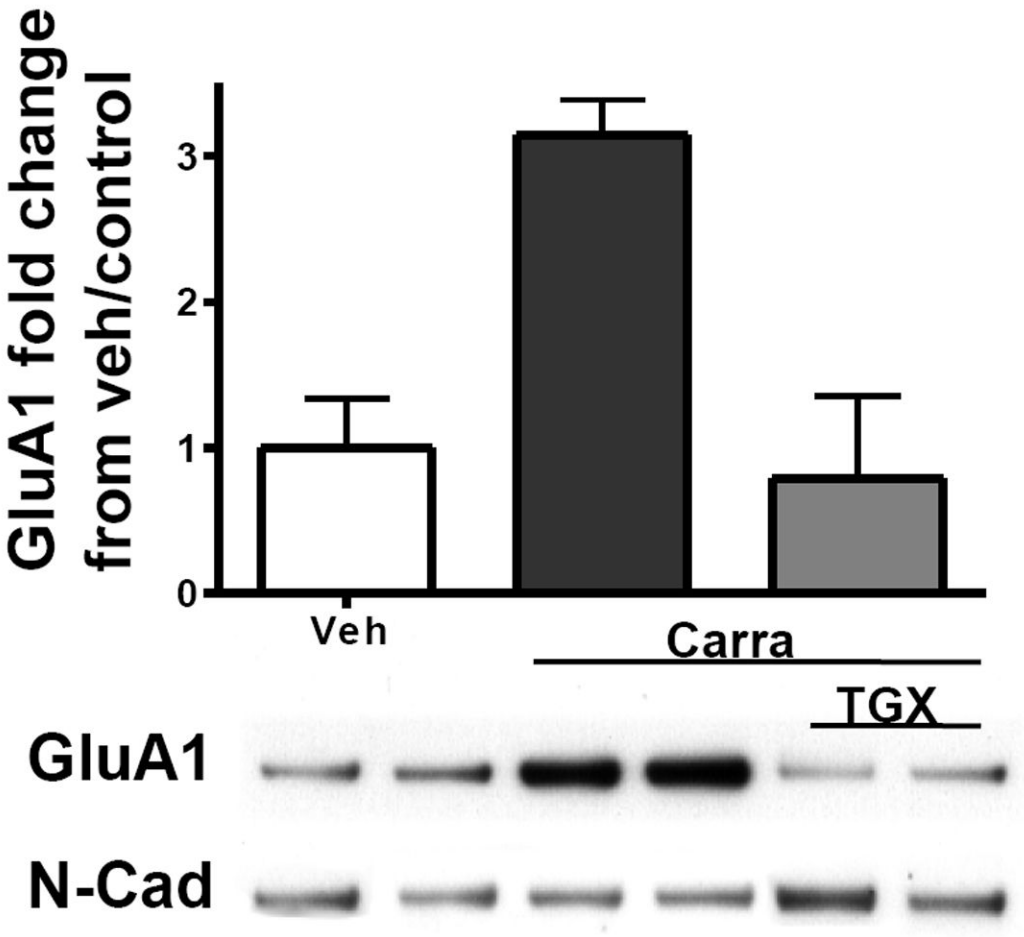

Figure 7.

Intraplantar carrageenan induced a mean 3 fold increase in GluA1, in membrane fractions of ipsilateral dorsal spinal cord. This was totally abrogated by i.t. pre-treatment with TGX 211 (1.8 μg). Two sample blots, including their N-Cad loading controls, are shown beneath each histogram bar. N= 3-4/group, * $p \leq 0.01$.

Table I

Relative Expression Units of mRNA in Naïve and Carrageenan-Treated Rats

	PI3Kα		PI3Kβ		PI3Kδ		PI3Kγ	
Spinal Cord	**Naive**	**Carra**	**Naïve**	**Carra**	**Naïve**	**Carra**	**Naïve**	**Carra**
mean	8.530	18.743	6.832	16.638	0.060	0.114*	2.807	1.110*
S.E.M.	4.83	3.07	4.60	1.96	0.01	0.02	0.65	0.30
	PI3Kα		**PI3Kβ**		**PI3Kδ**		**PI3Kγ**	
DRG	Naive	Carra	Naïve	Carra	Naïve	Carra	Naïve	Carra
mean	4.500	2.130*	2.833	1.150*	0.267	0.235	0.583	0.383
S.E.M.	0.68	0.59	0.24	0.36	0.10	0.04	0.21	0.12